

2D NMR Nutation Spectroscopy in Solids

A. SAMOSON AND E. LIPPMAN

*Institute of Chemical Physics and Biophysics of the Estonian Academy of Sciences,
Tallinn 200 001, USSR*

Received December 29, 1987

The quadrupole interaction parameters of half-integer spin nuclei are accessible from the dependence of NMR central transition magnetization on the RF excitation pulse length. These nutation spectra are obtained from spectral analysis of the magnetization amplitude and consist of up to $2I$ major lines. The lines correspond to central transition magnetization components, precessing in the plane perpendicular to the rotating magnetic field created by the RF excitation pulse. The magnetization components may be associated with single-quantum coherences in rotating magnetic field tilted by 90° from the strong stationary magnetic field. The precession direction differs for different transitions in the tilted frame and can be determined by an additional attenuated RF pulse, acting selectively on the central transition only. The RF field used must be as strong as possible. Increasing RF field strength leads to less complicated nutation spectra and facilitates their interpretation even under rapid magic-angle sample spinning conditions. © 1988 Academic Press, Inc.

Solid-state NMR spectroscopy is a valuable tool in the structural analysis of polycrystalline, glassy, and amorphous materials. The main spectroscopic parameter, the chemical shift, measures the response of a local electron cloud to the polarizing magnetic field and depends sensitively on the nature of the chemical bonding. Nuclei with spin $I > \frac{1}{2}$ possess quadrupole moments and interact with local electric field gradients, created by the charge distribution in the lattice. The electric quadrupole interaction is sensitive to local symmetry and vanishes if this symmetry is cubic. The quadrupole shifts, though informative, can cause significant lineform changes and broadening due to inherent anisotropy of the interaction. Interpretation of conventional MAS NMR spectra of quadrupolar nuclei is often complicated and sometimes impossible. New selective experimental techniques are needed to unravel such lines. Two-dimensional NMR nutation spectroscopy is the method of choice for this purpose. Information about the quadrupolar interactions is represented by shifts along an additional spectral axis, while shifts along the conventional spectral frequency axis are determined mainly by the chemical-shift interaction, if the polarizing magnetic field is strong enough and/or magic-angle sample spinning is applied. Two-dimensional NMR nutation spectroscopy of powders has already been applied to ^{11}B (1), ^{23}Na (2), ^{27}Al (3, 4), ^{45}Sc (5), ^{51}V (6), ^{55}Mn (7), ^{87}Rb (8), and ^{93}Nb (9). These experiments are related to various theoretical and structural problems, such as determination of quadrupolar interaction parameters with high-field sensitivity, unraveling of spectral lines from various sites, refinement of isotropic chemical shifts, and correlation of the anisotropies of chemical-shift and quadrupolar interaction tensors.

Qualitatively, detection of quadrupole modulation in the nutation spectra provides for the assignment of the observed lines, a prerequisite for quantitative interpretation of the NMR data.

Early papers on nutation (or excitation) spectroscopy presented only general principles of the phenomena involved (2, 10). Subsequent publications appended relevant experimental evidence about the effects of spectral offset and relaxation (11), but theoretical analysis has been confined to spin $I = \frac{3}{2}$ nuclei (7, 12).

Interpretation of experimental nutation spectra has been a matter of comparison with a set of simulated spectra (10, 11), calculated with the use of numerical matrix diagonalization algorithms. In this paper we present the analysis of pure nutation spectra and demonstrate the feasibility of an alternative approach, closer to the basic physics involved. Some important properties of the nutation process are demonstrated through the use of the new attenuated pulse technique, which may also serve for simplification of the spectra and development of 2D NMR quadrature detection.

THEORY

In the NMR spectroscopy of $I = \frac{3}{2}$, $\frac{5}{2}$, $\frac{7}{2}$, and $\frac{9}{2}$ half-integer spin nuclei only the central ($\frac{1}{2}$, $-\frac{1}{2}$) transition magnetization is usually recorded. Due to the absence of quadrupolar line broadening in first order, the central transition powder line is relatively narrow and can be selectively observed. The lines of other (satellite) transitions are shifted by quadrupolar interaction in first order (13) and the corresponding powder pattern lineshapes, representing all possible crystallite orientations, are broad and of correspondingly low amplitude.

In addition to the magnetic dipolar interactions, the central transition line may be both shifted and broadened by quadrupolar interaction in second order. Though the second order also carries full information about the quadrupolar interaction parameters, far more often it is just a nuisance leading to disturbing overlapping of spectral lines from different sites. The second-order effects decrease with increasing magnetic field strength and in a very high polarizing field only chemical shifts and other magnetic effects should remain. This ideal solution to the spectral resolution problem is, however, totally unrealistic within current magnet technology. One must measure the quadrupole couplings selectively and use the necessary corrections for chemical shifts. In order to mark the NMR lines corresponding to different magnetic shielding values with the appropriate quadrupolar interaction parameters, some modulation of the line amplitude or phase in the spirit of two-dimensional Fourier transform NMR spectroscopy is necessary. Generally, effects of the first-order quadrupolar splitting must be transferred to the detectable central transition coherence. One obvious way to do this is to use hard $\pi/2$ RF mixing pulses, separated by the parametric evolution time. The experimental realization of hard RF pulses, uniform over the whole spectral range, is technically difficult at best and generally impossible. A different and much more practical approach is to change the quantization axis of the nuclear spin for the whole evolution period. This has been done by reducing the strong magnetic field (14) and by application of a perpendicular rotating magnetic field (the RF pulse) (2). As was shown in Refs. (2-11), nutation of the central transition magnetization about the strong RF magnetic field is modulated by the quadrupo-

lar interaction. A subsequent Fourier analysis of the central transition signal amplitude time dependence yields the quadrupolar nutation spectrum, the nature of which we shall now study in detail.

We shall use explicit density-matrix formalism for theoretical evaluations. Several new techniques, based on the representation of spin-density-matrix elements by spherical tensor operators, have recently been developed in order to ease the analytical manipulations (15, 16). The new formalisms have been designed to evaluate the total single-quantum dipolar coherence as an observable. This is not suitable for nutation spectroscopy, where the central transition coherence is observed as a sum of contributions from all possible multiple coherences.

It is sufficient to consider a two-term spin Hamiltonian

$$\mathcal{H} = -\omega_{\text{RF}} I_x + \omega_{\text{Q}} (3I_z^2 - I^2), \quad [1]$$

where ω_{RF} is the RF field amplitude and

$$\omega_{\text{Q}} = \omega_{\text{Q}}^{\text{max}} \{ 1 - \sin^2 \beta [1 + \frac{1}{2}(1 - \eta \cos 2\alpha)] \} \quad [2]$$

is the quadrupolar splitting with the maximum value

$$\omega_{\text{Q}}^{\text{max}} = \frac{e^2 q Q}{4I(2I - 1)h}. \quad [3]$$

The orientation of the strong polarizing magnetic field in the principal axis system is given by the Euler angles $(\alpha, \beta, 0)$.

The Hamiltonian [1] describes very satisfactorily real spin systems in a strong polarizing magnetic field, where the Larmor frequency ω_{L} is large,

$$\omega_{\text{L}} \gg \omega_{\text{Q}}, \omega_{\text{RF}}, \quad [4]$$

and the weaker dipolar spin interactions with different rotational symmetry properties can be disregarded. In the I_z eigenfunction $|m\rangle$, ($m = I, \dots, -I$) basis the Hamiltonian [1] is represented by a $(2I + 1) \times (2I + 1)$ three-diagonal symmetric matrix. This matrix can be factored by choosing a different basis

$$|\pm \bar{m}\rangle = (|m\rangle \pm |-m\rangle) / \sqrt{2}, \quad m = \frac{1}{2}, \frac{3}{2}, \dots, I. \quad [5]$$

In this basis the Hamiltonian [1] is represented by two three-diagonal symmetric blocks, while

$$\bar{\mathcal{H}}_{1/2, -1/2} \equiv \langle \frac{1}{2} | \mathcal{H} | -\frac{1}{2} \rangle = \bar{\mathcal{H}}_{-1/2, 1/2} = 0. \quad [6]$$

Both blocks have $(I + \frac{1}{2}) \times (I + \frac{1}{2})$ dimension and differ only in one diagonal element, namely

$$\bar{\mathcal{H}}_{\pm 1/2, \pm 1/2} = \mp \frac{1}{2} (I + \frac{1}{2}) \omega_{\text{RF}} + [\frac{3}{4} - I(I + 1)] \omega_{\text{Q}}. \quad [7]$$

Other diagonal elements remain

$$\bar{\mathcal{H}}_{m, m} = \bar{\mathcal{H}}_{-m, -m} = \omega_{\text{Q}} [3m^2 - I(I + 1)], \quad m = \frac{3}{2}, \dots, I. \quad [8]$$

The equilibrium spin density matrix

$$\rho(0) = b_0 I_z, \quad \text{where} \quad b_0 = \frac{\hbar \omega_L}{k_0 T_0 (2I + 1)} \quad [9]$$

has in the $|\pm \bar{m}\rangle$ basis [5] the elements

$$\bar{\rho}_{m,-n}(0) = \bar{\rho}_{-n,m}(0) = bm, \quad m = n = \frac{1}{2}, \dots, I. \quad [10]$$

Both blocks of the factored Hamiltonian matrix $\bar{\mathcal{H}}_{m,n}$ can be separately diagonalized with two $(I + \frac{1}{2}) \times (I + \frac{1}{2})$ unitary matrices \mathbf{Z}

$$\bar{\mathcal{H}}_{\pm n, \pm n}^d = \mathbf{Z}_{\pm n, \pm k}^{-1} \bar{\mathcal{H}}_{\pm k, \pm l} \mathbf{Z}_{\pm l, \pm n}, \quad k, l, n = \frac{1}{2}, \dots, I, \quad [11]$$

which simplifies the analytical solution for the equation of motion of $I = \frac{5}{2}$ (17) and $I = \frac{7}{2}$ spins.

Evolution of the density matrix in the diagonalizing frame is given by a solution of the Liouville-von Neumann equation

$$\bar{\rho}_{k,-l}^d(t_1) = (\bar{\rho}_{-l,k}^d(t_1))^* = b_0 e^{-i\omega_{k,-l} t_1} \sum_{m=\frac{1}{2}}^I Z_{mk} Z_{-m,-k} m \quad [12]$$

and is governed by $(I + \frac{1}{2})^2$ eigenfrequencies

$$\omega_{k,-l} = \bar{\mathcal{H}}_{k,k}^d - \bar{\mathcal{H}}_{-l,-l}^d, \quad k, l = \frac{1}{2}, \dots, I. \quad [13]$$

Reversing the transformation [11] for the density matrix [12] and using [5] we finally obtain formal expressions for the central transition coherence

$$\begin{aligned} \rho_{1/2,-1/2}(t_1) &= \frac{1}{2} [\bar{\rho}_{1/2,1/2}(t_1) - \bar{\rho}_{1/2,-1/2}(t_1) + \bar{\rho}_{-1/2,1/2}(t_1) - \bar{\rho}_{-1/2,-1/2}(t_1)] \\ &= \rho_{-1/2,1/2}^*(t_1) = i \sum_{k,l=\frac{1}{2}}^I R_{k,-l} \sin \omega_{k,-l} t_1, \end{aligned} \quad [14]$$

and for the polarization

$$\begin{aligned} \rho_{1/2,1/2}(t_1) &= -\rho_{-1/2,-1/2}(t_1) \\ &= \sum_{k,l=\frac{1}{2}}^I R_{k,-l} \cos \omega_{k,-l} t_1, \end{aligned} \quad [15]$$

where the coefficients are calculated as

$$R_{k,-l} = b_0 \mathbf{Z}_{1/2,k} \mathbf{Z}_{-1/2,-l} \sum_{m=\frac{1}{2}}^I \mathbf{Z}_{m,k} \mathbf{Z}_{-m,-l} m. \quad [16]$$

The above expressions [14] and [15] could be simplified due to the symmetry of the Hamiltonian, resulting in

$$\bar{\rho}_{\pm 1/2, \pm 1/2}(t_1) = 0. \quad [17]$$

It follows from [14] and [15] that the central transition magnetization may be regarded as a sum of $(I + \frac{1}{2})^2$ magnetization vectors with amplitudes equal to $R_{k,-l}$ and rotating in the yz plane at frequencies equal to $\omega_{k,-l}$.

In the limit of a strong quadrupolar interaction

$$|\omega_Q| \gg \omega_{RF} \quad [18]$$

the Hamiltonian $\tilde{\mathcal{H}}$ is approximately diagonal in the $|\bar{m}\rangle$ basis [5] and the central transition magnetization is weakly modulated by the rotating components

$$\omega_{k,-l} = 3\omega_Q(k^2 - l^2), \quad \begin{cases} k, l = \frac{1}{2}, \dots, I \\ k \neq \frac{1}{2}, \quad l \neq \frac{1}{2}. \end{cases} \quad [19]$$

If $k = l$, then the modulation frequencies approach zero with the exception of the well-known component at

$$\omega_{1/2,-1/2} = -(I + \frac{1}{2})\omega_{RF} \quad [20]$$

with a high amplitude

$$R_{1/2,-1/2} = \frac{1}{2}b_0. \quad [21]$$

The physical origin of the rotating magnetization vectors with the frequencies $\omega_{k,-l}$ and amplitudes $R_{k,-l}$ may be better understood by regarding the evolution of the spin state in a tilted rotating frame. The coordinate transformation is just a 90° tilt of the rotating frame about the y axis. In this frame the RF magnetic field determines the axis of quantization.

The Hamiltonian modified as

$$\begin{aligned} \tilde{\mathcal{H}} &= e^{i\pi/2I_y} \mathcal{H} e^{-i\pi/2I_y} \\ &= -\omega_{RF} \tilde{I}_z - \frac{\omega_Q}{2} [3\tilde{I}_z^2 - I^2 + \frac{3}{2}(\tilde{I}_+^2 + \tilde{I}_-^2)] \end{aligned} \quad [22]$$

conserves the secular part of the quadrupole interaction, though with a twofold reduced magnitude. The equilibrium density matrix contains single-quantum coherences, as if created by an infinitely strong $\pi/2$ RF pulse

$$\tilde{\rho}(0) = -b_0 \tilde{I}_x. \quad [23]$$

The evolution of the spin density matrix proceeds to the first approximation (secular part only) in full analogy with the free induction decay in a strong time-independent magnetic field, except that the Zeeman interaction is proportional to the rotating magnetic field. The nonzero density-matrix elements are

$$\begin{aligned} \rho_{m,m-1}(t_1) &= -\frac{1}{2}b\sqrt{I(I+1) - m(m-1)} \exp\{i[\omega_{RF} + 3\omega_Q(m - \frac{1}{2})]t_1\}, \\ m &= I, \dots, -I + 1. \end{aligned} \quad [24]$$

All $2I$ tilted frame single transition coherences [24] modulate the rotating frame central transition coherence and polarization, with coefficients determined by the reduced Wigner rotation matrices $\mathbf{d}_{mn}^I(\pi/2)$ (18) as

$$\begin{aligned} \rho_{m,n}(t_1) &= \mathbf{d}_{m,k}^I(\pi/2) \tilde{\rho}_{k,k-1}(t_1) \mathbf{d}_{n,k-1}^I(\pi/2) + \mathbf{d}_{m,k-1}^I(\pi/2) \tilde{\rho}_{k-1,k}(t_1) \mathbf{d}_{n,k}^I(\pi/2), \\ m, n &= \frac{1}{2}, -\frac{1}{2}. \end{aligned} \quad [25]$$

TABLE I

Amplitudes $R_{k,-l}/b_0$ of the Central Transition Magnetization Components in the Strong RF Field Limit

I	$ \omega_{k,-l} $				
	ω_{RF}	$\omega_{RF} \pm 3\omega_Q$	$\omega_{RF} \pm 6\omega_Q$	$\omega_{RF} \pm 9\omega_Q$	$\omega_{RF} \pm 12\omega_Q$
$\frac{1}{2}$	$-\frac{1}{2}$				
$\frac{3}{2}$	$\frac{2}{8}$	$-\frac{3}{8}$			
$\frac{5}{2}$	$-\frac{6}{16}$	$\frac{4}{16}$	$-\frac{5}{16}$		
$\frac{7}{2}$	$\frac{36}{128}$	$-\frac{45}{128}$	$\frac{30}{128}$	$-\frac{35}{128}$	
$\frac{9}{2}$	$-\frac{90}{256}$	$\frac{72}{256}$	$-\frac{84}{256}$	$\frac{56}{256}$	$-\frac{63}{256}$

The resulting $2I$ amplitudes $R_{k,-l}$ of the central transition magnetization components are presented in Table I. Directions of the nutations at frequencies $|\omega_{k,-l}|$ are determined by the signs of the corresponding amplitudes. For nuclei with spin $I = \frac{3}{2}$ evolution during the RF pulse may be visualized as shown in Fig. 1.

The other $(I - \frac{1}{2})^2$ central transition magnetization components may be considered multiple-quantum coherences in the tilted frame created by the nonsecular part of the Hamiltonian [22]. The \tilde{I}_{\pm}^2 operators create in the tilted frame only odd-quantum coherences, thus complementing the number of possible nutating components of the

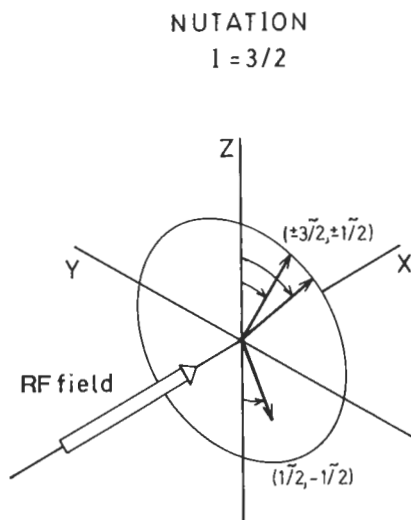


FIG. 1. Evolution of the central transition magnetization components during the RF pulse for spin $I = \frac{3}{2}$. Individual magnetization components are associated with single-quantum transitions in the tilted rotating frame.

rotating frame central transition magnetization up to $(I + \frac{1}{2})^2$. The amplitudes of these components may be assumed small according to the perturbation theory. The first moment about the origin $F_1 = 0$ of the nutation spectrum is proportional to the number of resonating nuclei and serves for quantitative interpretation of the spectra. As was shown for the $I = \frac{3}{2}, \frac{5}{2}$ nuclei in (2) and for the general case in (17), for small RF pulse flip angles $\omega_{RF}t_1 \rightarrow 0$ the intensity of the central transition coherence does not depend upon the magnitude of the quadrupole splitting ω_Q (unless $\omega_Q > \omega_L$) and

$$\rho_{1/2,-1/2}(t_1) = -\frac{i}{2} b_0 (I + \frac{1}{2}) \omega_{RF} t_1. \quad [26]$$

Indeed, it follows from [14] and [26] that for $t_1 \rightarrow 0$ the first moment about the origin approaches the limiting value

$$\sum_{k,l=\frac{1}{2}}^I R_{k,-l} \omega_{k,-l} = \frac{1}{2} b_0 (I + \frac{1}{2}) \omega_{RF}, \quad [27]$$

independent of ω_Q .

It also follows from [26] that for the two limiting cases of small $\omega_Q = 0$ and large quadrupole coupling $\omega_Q \gg \omega_{RF}$ [21], the ratio of the first moment to the integral amplitude of an NMR line, i.e., the line center of gravity (CG), is a monotonous function of the relative quadrupolar splitting ω_Q/ω_{RF}

$$\text{CG} = \frac{\sum_{k,l=\frac{1}{2}}^I R_{k,-l} \omega_{k,-l}}{\sum_{k,l=\frac{1}{2}}^I |R_{k,-l}|} \begin{cases} = \omega_{RF} & \text{if } \omega_Q = 0 \ll \omega_{RF} \\ = (I + \frac{1}{2}) \omega_{RF} & \text{if } \omega_Q \gg \omega_{RF}. \end{cases} \quad [28]$$

DISCUSSION

Numerical calculations on a Cadmus 9900 computer of the central transition magnetization components corroborate all the theoretical considerations presented in the sine-transform spectra of the central transition coherence $\rho_{1/2,-1/2}(t_1)$ for the four possible half-integer spin values as a function of the relative quadrupole splitting ω_Q/ω_{RF} .

For $|\omega_Q| < \frac{1}{10} \omega_{RF}$, the $2I - 1$ nutating magnetization components are shifted in linear dependence on the ω_Q/ω_{RF} ratio, as predicted by [24]. One line, ascribed to the central transition in the tilted frame, remains at ω_{RF} .

In the limit of a large quadrupole splitting $|\omega_Q| \gg \omega_{RF}$, the frequencies either increase with ω_Q or approach zero in accordance with the combination of the quantum numbers in [19]. Only one component, assigned to the highest satellite transition in the tilted rotating frame, conserves a regular amplitude and frequency.

The lines, located for $\omega_Q \ll \omega_{RF}$ symmetrically about $n\omega_{RF}$, $n = 3, 5, \dots, 2I$, represent multiquantum transitions in the tilted frame and remain weak throughout the whole range of possible quadrupole splittings ω_Q .

The graphs given in Figs. 2-5 together with the known dependence of the quadrupole splittings ω_Q on the Euler orientation angles allow easy interpretation and visualization of the nutation spectra of powder samples (see Fig. 6) and provide a means

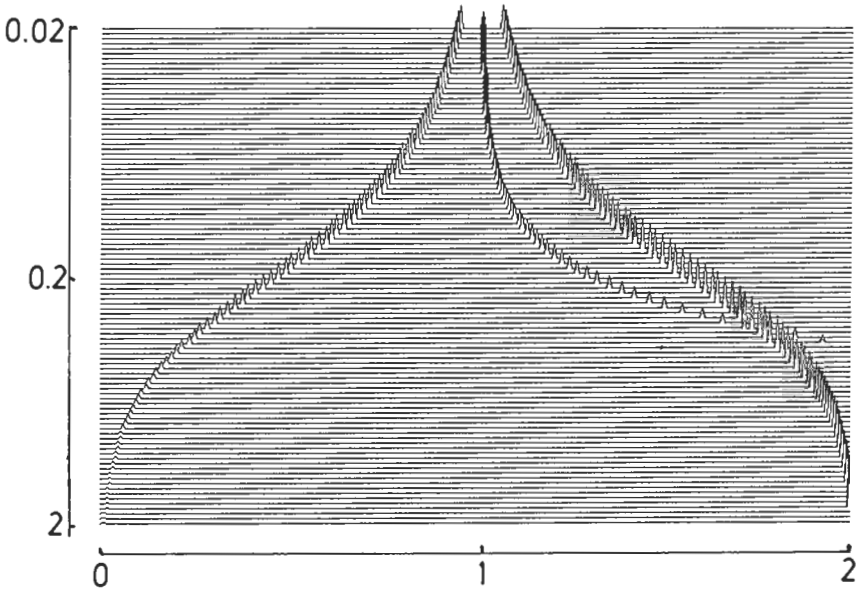


FIG. 2. Dependence of the nutation frequencies $|\omega_{k,-l}|$ (horizontal axis) on the ω_Q/ω_{RF} ratio (vertical logarithmic axis) for spin $I = \frac{3}{2}$. The horizontal axis is scaled in the multiples of ω_{RF} .

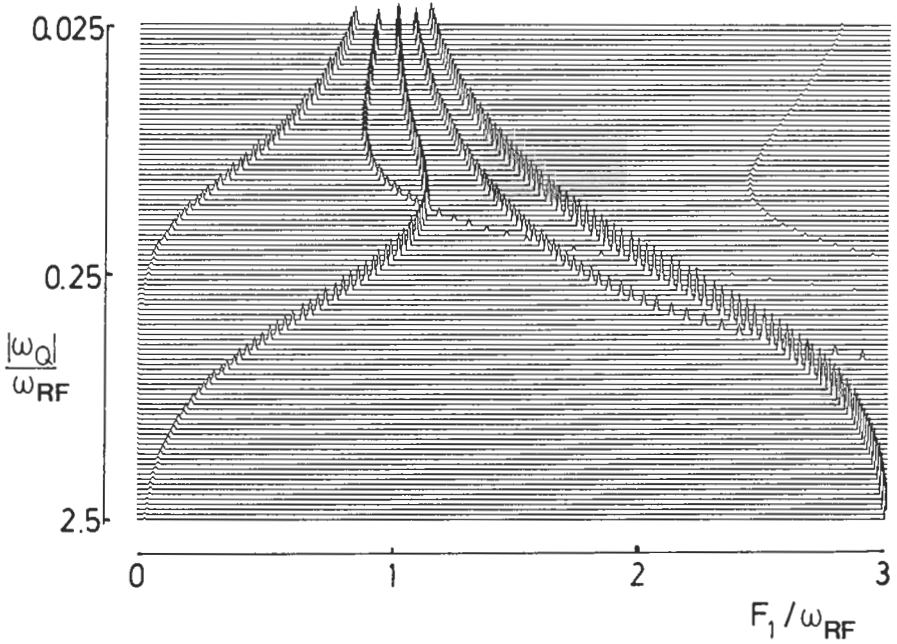


FIG. 3. Same as Fig. 2, for spin $I = \frac{5}{2}$.

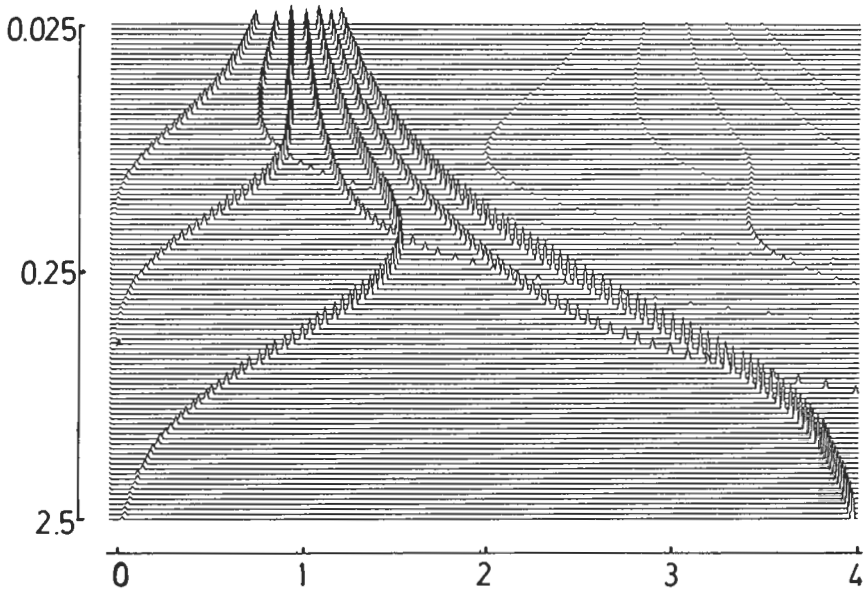


FIG. 4. Same as Fig. 3, for spin $I = \frac{7}{2}$.

for two-dimensional correlation of the quadrupole interaction with the chemical-shift anisotropy (6). Note that twofold singularities appear in the powder pattern nutation spectra. The first are analogous to those in the broad line NMR spectra and depend

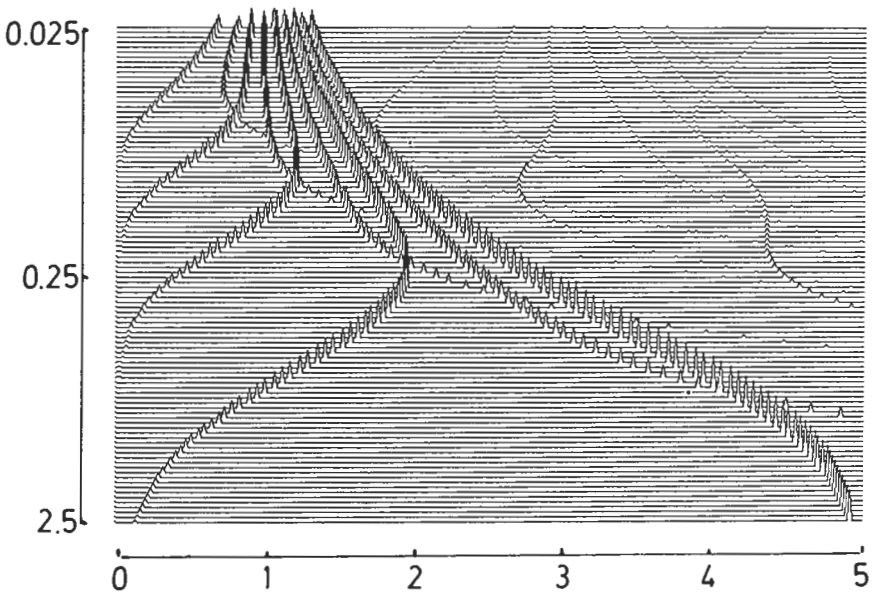


FIG. 5. Same as Fig. 4, for spin $I = \frac{9}{2}$.

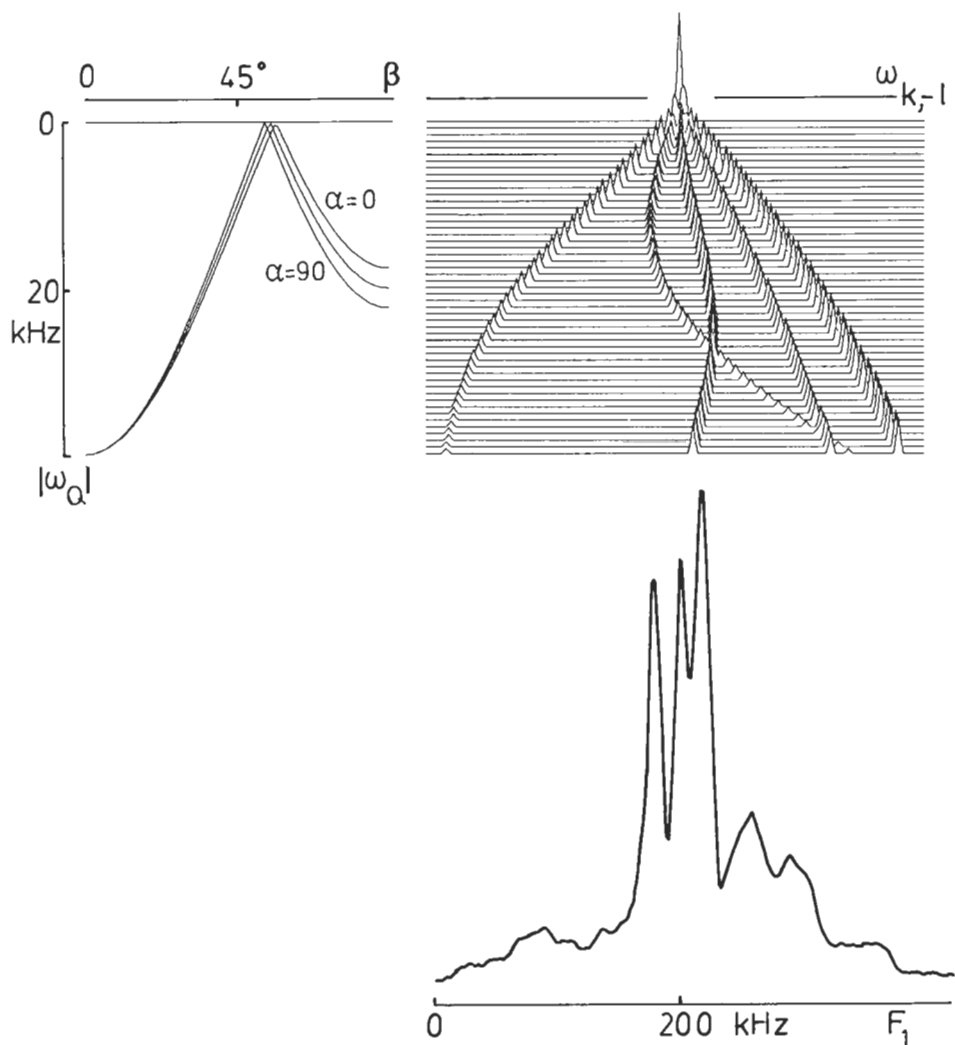


FIG. 6. The powder sample nutation spectrum of ^{55}Mn ($I = \frac{5}{2}$) in KMnO_4 at 90 MHz (bottom figure). The quadrupole interaction constant $e^2qQ/h = 1.6$ MHz ($2I$) ($\omega_Q^{\text{max}} = 40$ kHz) determines the total width of the nutation spectrum with components shown at upper right to the same scale. The narrow peaks near $\omega_{\text{RF}} = 200$ kHz are caused by the zero derivative [29], as is clearly evident from the superposed figures. Other features in the powder pattern are determined by orientational distribution of the sample particles. Three tilted frame satellite transition singularities determined by $|\omega_Q| = |\omega_Q(\alpha = 0^\circ, \beta = 90^\circ)|$ and a shoulder due to nonzero asymmetry $\eta = 0.1$ ($\alpha = 90^\circ$) are prominent in the experimental spectrum.

on the quadrupole interaction parameters e^2qQ/h and η . The relative positions of additional peaks, located at

$$F_1 = \omega_{k,-l}; d\omega_{k,-l}/d\omega_Q = 0, \quad [29]$$

are independent of a particular quadrupole coupling value and may change only in

amplitude. In case of a relatively large quadrupolar interaction the powder sample nutation spectrum shifts toward $(I + \frac{1}{2})\omega_{RF}$ [28] with little variation in the highest frequency. A more reliable spectral parameter for the determination of the quadrupole interaction constant is then the center of gravity of the powder lineshape ω_{CG}^P , which can be obtained from [28] by averaging over all possible orientations of the crystallite (see Fig. 7).

The opposite nutation directions of the central transition magnetization components provide new possibilities for the interpretation of nutation spectra. The direction of nutation manifests itself in the z component [15] of the total central transition polarization. Depending upon the number of the associated satellite transitions in the tilted frame, this amplitude may have a positive or negative value (see Table 1). The polarization of the central transition magnetization can be converted into transverse magnetization with an additional, selective $\pi/2$ RF pulse. The necessary selectivity (action only) on the central transition can be achieved by attenuation of the strong excitation pulse. We detected opposite contributions to the central transition polarization from the tilted frame satellite and central transitions of a $I = \frac{1}{2}$ spin (see Fig. 8).

Obviously, various schemes of sophisticated 2D NMR Fourier spectroscopy can be realized with selective RF pulses of an attenuated amplitude, resulting in quadrature spectra in both spectral dimensions. This approach is especially suitable for sorting out some particular straight branches of the tilted frame transitions or for suppressing the zero-frequency peaks due to offset effects (5). The straight branches form peaks in the nutation spectrum at frequencies that depend linearly on the magnitude of the quadrupole coupling constant, as shown in Fig. 6.

The tilted frame formalism also allows the evaluation of the effect on the nutation spectra of magic-angle sample spinning. Since the basis transformations are independent of ω_Q , only a modulation of the transition frequencies by sample spinning is to be expected. This modulation comes about through the spinning-generated time

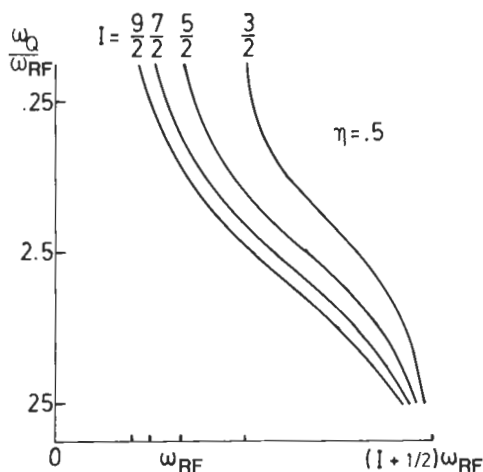


FIG. 7. Shifts of the center of gravity of the powder sample nutation spectra for $\eta = 0.5$.



FIG. 8. The y and z components of the central transition magnetization of ^{23}Na ($I = \frac{3}{2}$) in NaNO_3 ($e^2qQ/h = 334$ kHz (13)) at 53 MHz. The spin state evolution is determined by the x pulse ($\omega_{\text{RF}} = 180$ kHz). The z component of the central transition magnetization is rotated into the x, y plane selectively with an additional attenuated 90° pulse ($\omega_{\text{RF}} = 10$ kHz) of the same frequency. The experimental spectra were registered on Bruker Physik CXP-series NMR spectrometers at 4.7 and 8.4 T.

dependence of the Euler angles in the formula for the quadrupole splitting ω_Q . Despite a twofold reduction, the quadrupole powder pattern linewidth in the tilted frame is usually still large in comparison to the sample spinning frequency. If the total spin state evolution time t_1 is short relative to the sample spinning period, then a reasonably faithful reproduction of the powder sample nutation spectrum lineshape can still be achieved. In order to avoid destructive interference of the spinning-dependent phase of the magnetization vector (19), the strong RF pulse duration t_1 should be less than a quarter of the sample spinning period

$$t_1 \leq \omega_{\text{rot}}^{-1}/4. \quad [30]$$

Though for some particular crystallites this condition may still produce large deviations in the signal phase, these disturbing contributions tend to cancel in a polycrystalline sample. Recent theoretical work (20) on transition to a static limit is in line with the present argument. The condition [30] seems very restrictive in terms of the powder sample nutation lineshape spectral resolution, but in fact it still allows recording the nutation spectra with sufficient detail. A numerical simulation indicates that the powder sample nutation spectrum lineshape of the first satellite transition in the tilted frame is still readily recognizable even if $\omega_Q/\omega_{\text{rot}} < 10$, as shown in Fig. 9. The situation is even more favorable for the next satellite transition with a broader line.

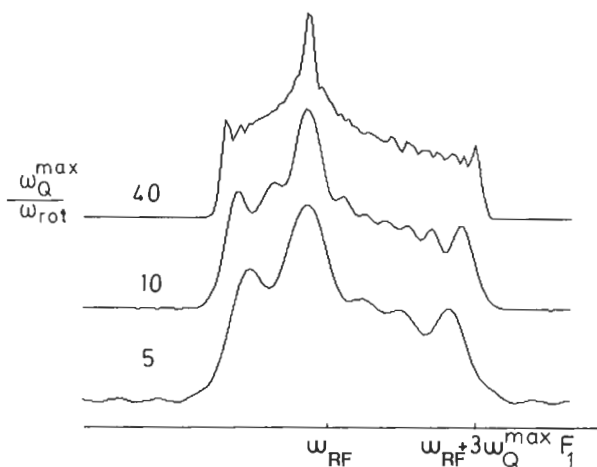


FIG. 9. The powder pattern lineshapes of the first satellite transition in the tilted frame as a function of the $\omega_Q^{\max}/\omega_{rot}$ ratio. The relative resolution increases with increasing spin state development time t_1 , equal to $\approx \frac{1}{4}$ of the sample rotation period in all cases.

CONCLUSIONS

Fourier analysis of the central transition signal amplitude as a function of the strong RF excitation pulse duration t_1 yields a nutation spectrum, consisting of at most $2I$ lines. The first moment of this spectrum about the origin is proportional to the number of resonating nuclei. If the RF field during the pulse is of a strength comparable to the first-order quadrupolar splitting, then the lines in the nutation spectrum may be associated with single-quantum transitions in a rotating magnetic field. The nutation directions and amplitudes manifest themselves in the central transition coherence and polarization and have opposite signs for neighboring tilted frame transitions. The central transition polarization can be made detectable with an attenuated $\pi/2$ RF pulse, selective for the central transition. Even the hypercomplex Fourier transform technique may be realized with a suitable choice of the phases of the strong and attenuated RF pulses. Any increase in the RF pulse strength facilitates interpretation of the powder sample nutation spectra, especially if magic-angle spinning is used.

REFERENCES

1. D. MÜLLER, Bruker Report, Vol. 2, p. 20, 1986.
2. A. SAMOSON AND E. LIPPMAA, *Phys. Rev. B* **28**, 6567 (1983).
3. E. LIPPMAA, A. SAMOSON, AND M. MÄGI, *J. Am. Chem. Soc.* **108**, 1730 (1986).
4. A. SAMOSON, E. LIPPMAA, G. ENGELHARDT, U. LOHSE, AND H.-G. JERSCHKEWITZ, *Chem. Phys. Lett.* **134**, 589 (1987).
5. A. P. M. KENTGENS, J. J. M. LEMMENS, F. M. M. GEURTS, AND W. S. VEEMAN, *J. Magn. Reson.* **71**, 63 (1987).
6. A. SAMOSON AND V. MIIDEL, "IXth AMPERE Summer School, Abstracts, Novosibirsk, 1987," p. 113.
7. P. P. MAN, *J. Magn. Reson.* **67**, 78 (1986).

8. A. TROKINER, P. P. MAN, H. THEVENEAU, AND P. PAPON, *Solid State Commun.* **85**, 929 (1985).
9. P. P. MAN, H. THEVENEAU, AND P. PAPON, *J. Magn. Reson.* **64**, 271 (1985).
10. A. SAMOSON AND E. LIPPMAA, *Chem. Phys. Lett.* **100**, 205 (1983).
11. F. M. M. GEURTS, A. P. M. KENTGENS, AND W. S. VEEMAN, *Chem. Phys. Lett.* **120**, 206 (1985).
12. A. WOKAUN AND R. R. ERNST, *J. Chem. Phys.* **67**, 1752 (1977).
13. R. POUND, *Phys. Rev.* **79**, 685 (1950).
14. D. P. WEITEKAMP, A. BIELECKI, D. B. ZAX, K. W. ZILM, AND A. PINES, *Phys. Rev. Lett.* **50**, 1807 (1983).
15. B. C. SANCTUARY, T. K. HALSTEAD, AND P. A. OSMENT, *Mol. Phys.* **49**, 753 (1983).
16. B. C. SANCTUARY, *Mol. Phys.* **49**, 785 (1983).
17. A. SAMOSON, Ph.D. theses (Tallinn, 1984).
18. D. A. VARSHALOVITCH, A. N. MOSKALEV, AND V. K. KHERSONSKII, "Kvantovaja teorija uglovovo momenta," Nauka, Leningrad, 1975.
19. A. SAMOSON, E. KUNDLA, AND E. LIPPMAA, *J. Magn. Reson.* **49**, 350 (1982).
20. M. MUNOWITZ, *J. Magn. Reson.* **73**, 338 (1987).
21. M. WADSWORTH AND P. FRANCE, *J. Magn. Reson.* **51**, 424 (1983).